Inorganic Chemistry

Article

Tuning the Coordination Geometry of Silver in Bis(pyrazolyl)alkane Complexes

Daniel L. Reger,* James R. Gardinier, and Mark D. Smith

Department of Chemistry and Biochemistry, University of South Carolina, Columbia, South Carolina 29208

Received March 4, 2004

Silver(I) complexes of the bis(pyrazolyl)methane ligands $Ph_2C(pz)_2$, $PhCH(pz)_2$, and $PhCH_2CH(pz)_2$ (pz = pyrazolyl ring) have been prepared in an attempt to explore how sterically hindered poly(pyrazolyl)methane ligands influence the variable coordination geometries exhibited by silver(I) complexes, especially its ability to participate in cation$\cdots\pi$ interactions. The complex $\{Ag[(pz)_2CPh_2]_2\}(PF_6)\cdot C_3H_6O$ adopts an unusual square planar coordination environment as indicated by the sum of the four N–Ag–N angles being 360°. The proximity of phenyl groups above and below the AgN_4 core enforces the unusual coordination geometry about the metal center. This arrangement is not a result of silver(I)$\cdots\pi$ arene interactions but rather of the constraints imposed by the steric crowding caused by $(aryl)_2C(pz)_2$ ligands. In contrast, the complexes of the other two ligands, $\{Ag[(pz)_2CHPh]_2\}(PF_6)\cdot 0.5CH_2Cl_2$ and $\{Ag[(pz)_2CH(CH_2Ph)]_2\}(PF_6)\cdot CH_2Cl_2$, show normal tetrahedral geometry about the silver(I), also with no indication of silver(I)$\cdots\pi$ arene interactions. All three new complexes have extended supramolecular structures supported by a combination of CH$\cdots\pi$ and CH$\cdots$F interactions.

Introduction

It is of fundamental and practical[1] interests to more fully understand what factors govern whether a cation$\cdots\pi$ interaction will take place when the components are brought into close proximity. One common approach to preparing compounds capable of becoming involved in a cation$\cdots\pi$ interaction is to have multiple Lewis bases tethered to a central arene core where the donors serve to anchor the metal cation close to the π-cloud of the ring (Figure 1). This strategy, coupled with the use of noncoordinating anions to render the metal centers more "electron deficient", may promote but does not guarantee the occurrence of a cation$\cdots\pi$ interaction (as typically quantified by X-ray structural data and/or spectroscopic methods; vide infra).

Our group recently reported the structure of a silver poly-(pyrazolyl)methane coordination polymer, $\{o$-$C_6H_4[CH_2$-$OCH_2C(3$-$Phpz)_3]_2Ag_2(acetone)(BF_4)_2\}_n$ (pz = pyrazolyl ring), that exhibited an η^2-cation$\cdots\pi$ interaction between the
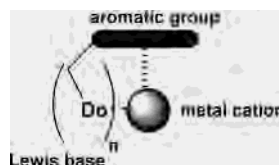
**Figure 1.** Typical framework used for studying metal cation$\cdots\pi$ complexes.

metal center and a 3-phenyl group bound to a pyrazolyl ring of an adjacent cation.[2] We also recently described the preparation of a new bitopic fixed geometry heteroscorpionate, m-$C_6H_4[C(pz)_2(2$-$py)]_2$ (py = pyridyl ring), and its corresponding silver hexafluorophosphate complex, $\{Ag(\kappa^2$-m-$C_6H_4[C(pz)_2(2$-$py)]_2)_2\}(PF_6)$.[3] One striking feature about this latter complex was a square planar arrangement of nitrogen atoms from coordinated pyrazolyl groups about the silver(I) center where the uncoordinated pyridyl groups sandwiched the metal center. The compound $\{Ag(\kappa^2$-C_6H_5-$[C(pz)_2(2$-$py)]_2)_2\}(PF_6)$[3] showed a similar square planar arrangement of donor atoms about silver; however, phenyl groups rather than pyridyls sandwiched the metal center. We proposed that the atypical coordination geometry of tetra-

---

* Author to whom correspondence should be addressed. E-mail: reger@mail.chem.sc.edu.

(1) For instance, in metal cation sensors: Xu, F.-B.; Li, Q.-S.; Wu, L.-Z.; Leng, X.-B.; Li, Z.-C.; Zeng, X.-S.; Chow, Y. L.; Zhang, Z.-Z. *Organometallics* **2003**, *22* (4), 633. (b) de Silva, A. P.; Gunaratne, H. Q. N.; Gunnlaugsson, T.; Huxley, A. J. M.; McCoy, C. P.; Rademacher, J. T.; Rice, T. E. *Chem. Rev.* **1997**, *97* (5), 1515. Fabbrizzi, L.; Poggi, A. *Chem. Soc. Rev.* **1995**, *24* (3), 197.

(2) Reger, D. L.; Semeniuc, R. F.; Smith, M. D. *Inorg. Chem. Commun.* **2002**, *5*, 278.

(3) Reger, D. L.; Gardinier, J. R.; Smith, M. D. *Polyhedron* **2004**, *23* (2−3), 291.
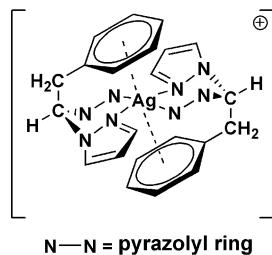
Figure 2. Possible cation···π interaction in {Ag[(pz)$_2$CHCH$_2$Ph]$_2$}$^+$, where some carbon and hydrogen atoms of two pz rings have been omitted for clarity.

coordinate silver(I) in these complexes was due to inter-cationic CH···F interactions involving the arene substituents of the ligands and the fluorines of the hexafluorophosphate salts rather than to any intracationic Ag···π or CH···π interactions. To more fully elucidate the factors that were responsible for the unusual coordination environment about silver in the *solid state structures* of the above bidentate scorpionates and to probe the possibility of obtaining species with short cation···π interactions, we investigated silver complexes of the bis(pyrazolyl)methane ligands Ph$_2$C(pz)$_2$ (**L^1**), PhCH(pz)$_2$ (**L^2**), and PhCH$_2$CH(pz)$_2$ (**L^3**). The latter ligand was thought to be capable of promoting a silver···arene interaction due to the flexibility of the ligand backbone as in Figure 2.

Experimental Section

General Considerations. Solvents for synthetic procedures and spectroscopic studies were dried by conventional methods and distilled under N$_2$ atmosphere immediately prior to use. All reagents were used as received from Aldrich Chemical Co. Silica gel (0.040−0.063 mm, 230−400 mesh) used for chromatographic separations was purchased from Fischer Scientific. PhCH$_2$CH(OEt)$_2$ (bp 85−88 °C, 1 mmHg) was prepared by an established method from Mg°, benzylbromide, and HC(OEt)$_3$.[4] Manipulation of AgPF$_6$ was carried out in an inert-atmosphere drybox or by using standard Schlenk techniques. After reaction of AgPF$_6$ with bis(pyrazolyl)-methane ligands, no special precautions are needed to handle the silver salts. Robertson Microlit Laboratories performed all elemental analyses. Melting point determinations were made on samples contained in sealed glass capillaries by using an Electrothermal 9100 apparatus and are uncorrected. Mass spectrometric measurements recorded in ESI(+) mode were obtained on a Micromass Q-Tof spectrometer whereas those performed by using direct probe analyses were made on a VG 70S instrument. NMR spectra were recorded by using either a Varian Gemini 300 or a Varian Mercury 400 instrument, as noted within the text. Chemical shifts were referenced to solvent resonances at δ_H 2.05 and δ_C 29.8 for acetone-d_6.

Ligand Syntheses. α,α-Diphenyl-α,α-bis(pyrazol-1-yl)methane, Ph$_2$C(pz)$_2$ (L^1). A Schlenk flask was charged with 5.00 g (21.0 mmol) of Ph$_2$CCl$_2$, 6.61 g (97.1 mmol) of pyrazole, 25 mL of NEt$_3$, and 50 mL of toluene, and the reaction mixture was heated at reflux for 3 d. Solvent was then removed by vacuum distillation, and the resulting pale yellow solid was washed with four 20 mL portions of methanol to leave 3.76 g (61% yield) of the desired ligand as a colorless solid. Mp: 158−159 °C (lit.[6b] mp 153−154 °C). ^{1}H NMR (400 MHz): 7.65 (d, J = 1 Hz, 2H, H$_3$-pz), 7.49 (d, J = 2 Hz, 2H,

H$_5$-pz), 7.45−7.36 (br m, 6H, Ph), 7.05 (d, J = 8 Hz, 4H, Ph), 6.36 (dd, J = 2,1 Hz, 2H, H$_4$-pz). ^{13}C NMR (100.6 MHz, acetone-d_6): 141.8, 140.6 (C$_5$-pz), 133.3, 130.0, 129.7 (C$_3$-pz), 128.6, 106.1 (C$_4$-pz), 88.3 (C$_\alpha$). HRMS-direct probe (m/z): [M]$^+$, calcd for C$_{19}$H$_{16}$N$_4$ 300.1375; found, 300.1367. Direct probe MS {m/z (rel int %), [assignment]$^+$}: 300 (35), [M]$^+$; 233 (100), [M − pz]$^+$; 223 (44), [M − Ph]$^+$; 166 (21), [M − 2pz]$^+$; 156 (13), [M − Ph − pz]$^+$; 77 (22), [C$_6$H$_5$]$^+$.

α,α-Bis(pyrazol-1-yl)toluene, PhCH(pz)$_2$ (L^2). PhCH(pz)$_2$ was prepared by a modification of the known route.[5] Thus, 15.2 g (0.100 mol) of PhCH(OMe)$_2$, 13.6 g (0.200 mol) of pyrazole, and 0.203 g (1.07 mmol) of p-toluenesulfonic acid monohydrate (p-TsOH·H$_2$O) were heated in a short-path distillation apparatus 12 h at atmospheric pressure until 7.1 mL (87% expected) of methanol was collected. The residue was partitioned between 100 mL each of H$_2$O and Et$_2$O. The organic and aqueous portions were separated, and the aqueous portion was extracted with three 100 mL portions of Et$_2$O. The combined organic fractions were dried over MgSO$_4$ and filtered, and solvent was removed by vacuum distillation. The residue was taken up with 100 mL of 1:1 (v/v) hexanes/Et$_2$O, and the solution was flushed through a silica gel plug to remove colored impurities. Solvent was removed, leaving a colorless solid that was washed with two 15 mL portions of hexanes and dried under vacuum to give 16.9 g (75%) of PhCH(pz)$_2$ as a colorless solid. Mp: 68−69 °C (lit. mp 61−62 °C,[6] 62−63 °C[7]). ^{1}H NMR (300 MHz): 7.95 (s, 1H, CH), 7.81 (d, J = 2 Hz, 2H, H$_5$-pz), 7.58 (d, J = 1 Hz, 2H, H$_3$-pz), 7.41−7.37 (br m, 3H, Ph), 7.09−7.05 (br m, 2H, Ph), 6.36 (dd, J = 2,1 Hz, 2H, H$_4$-pz). ^{13}C NMR (75.4 MHz): 140.8 (C$_5$-pz), 138.3 (C$_{ipso}$Ph), 130.8 (C$_{para}$), 129.7 (C$_3$-pz), 129.3 (C$_{ortho}$), 127.8 (C$_{meta}$), 106.9 (C$_4$-pz), 78.1 (C$_\alpha$). HRMS-direct probe (m/z): [M]$^+$ calcd for C$_{13}$H$_{12}$N$_4$, 224.1062; found, 224.1060. Direct probe MS {m/z (rel int %), [assignment]$^+$}: 224 (21), [M]$^+$; 157 (100), [M − pz]$^+$; 77 (16), [C$_6$H$_5$]$^+$.

α-Benzyl-α,α-bis(pyrazol-1-yl)methane, PhCH$_2$CH(pz)$_2$ (L^3). A mixture of 1.77 g (9.11 mmol) of PhCH$_2$CH(OEt)$_2$ and 1.24 g (18.2 mmol) of pyrazole and a catalytic amount (0.023 g, 0.12 mmol, 1 mol %) of p-TsOH·H$_2$O were heated in a short-path distillation apparatus for 8 h until 0.6 mL (60% of expected) of EtOH was collected. The residue was partitioned between 100 mL each of H$_2$O and Et$_2$O. The organic and aqueous portions were separated, and the aqueous portion was extracted with three 100 mL portions of Et$_2$O. After the organic portions were dried over MgSO$_4$ and filtered and solvent was removed, the resulting brown oil was loaded onto a silica gel column; grease and two impurities thought to be 1-(pyrazolyl)styrene and 1-(ethoxy)styrene (on the basis of the NMR spectra of the mixture) were removed by first eluting the column with C$_6$H$_6$. The column was then flushed with Et$_2$O to elute the desired product, which after removing solvent by vacuum distillation afforded 0.832 g (38% yield) of PhCH$_2$CH-(pz)$_2$ as a colorless solid. Mp: 105−107 °C (lit.[7] mp 107−108 °C). ^{1}H NMR (300 MHz): 7.86 (d, J = 2 Hz, 2H, H$_5$-pz), 7.58 (d, J = 1 Hz, 2H, H$_3$-pz), 7.22−7.16 (br m, 5H, Ph), 6.79 (t, J = 8 Hz, 1H, CH), 6.22 (dd, J = 2,1 Hz, 2H, H$_4$-pz), 3.91 (d, J = 8 Hz, 2H, CH$_2$). ^{13}C NMR (75.4 MHz, acetone-d_6): 140.2 (C$_5$-pz), 130.0, 129.7 (C$_3$-pz), 129.1, 127.6, 106.6 (C$_4$-pz), 77.1 (C$_\alpha$), 40.4 (CH$_2$).

(4) McElvain, S. M.; Clarke, R. L.; Jones, G. D. *J. Am. Chem. Soc.* **1942**, *64*, 1966.

(5) (a) Ballesteros, P.; Elguero, J.; Claramunt, R. M. *Tetrahedron* **1985**, *41* (24), 5955. (b) Ballaesteros, P.; Lopez, C.; Claramunt, R. M.; Jimenez, J. A.; Cano, M.; Heras, J. V.; Pinilla, E.; Monge, A. *Organometallics* **1994**, *13*, 289.

(6) (a) The, K. I.; Peterson, L. K. *Can. J. Chem.* **1973**, *51* (3), 422. (b) The, K. I.; Peterson, L. K.; Kiehlman, E. *Can. J. Chem.* **1973**, *51* (15), 2448.

(7) Katritzky, A. R.; Abdel-Rahman, A. E.; Leahy, D. E.; Schwarz, O. A. *Tetrahedron* **1983**, *39* (24), 4133.

HRMS-direct probe (m/z): [M]$^+$ calcd for $C_{14}H_{14}N_4$, 238.1218; found, 238.1223. Direct probe MS {m/z (rel int %), [assignment]$^+$}: 238 (7), [M]$^+$; 170 (34), [M − Hpz]$^+$; 147 (100), [(pz)$_2$CH]$^+$; 103 (13), [CHCHPh]$^+$; 91 (18), [H$_2$CPh$_2$]$^+$.

Silver Complexes. {Ag[(pz)$_2$CPh$_2$]$_2$}(PF$_6$) (1). A 5 mL THF solution of 0.38 g (1.3 mmol) of Ph$_2$C(pz)$_2$ was added to a 5 mL THF solution of 0.16 g (0.63 mmol) of AgPF$_6$ under a nitrogen atmosphere. A colorless precipitate formed within 10 min of stirring. The resulting suspension was stirred 4 h and then was separated by cannula filtration. The colorless solid was washed with 5 mL of Et$_2$O and dried under vacuum to leave 0.40 g (74% yield) of {Ag[(pz)$_2$CPh$_2$]$_2$}(PF$_6$) as a colorless solid. Mp: 215−218 °C (dec). Anal. Calcd (found) for $C_{38}H_{32}F_6N_8PAg$: C, 53.47 (53.78); H, 3.78 (3.86); 13.13 (12.83). ^{1}H NMR (400 MHz): 7.67 (d, J = 2 Hz, 4H, H$_5$-pz), 7.63−7.54 (br m, 12 H, Ph), 7.46 (d, J = 1 Hz, 4H, H$_3$-pz), 6.83 (d, J = 8 Hz, 8H, Ph), 6.49 (dd, J = 2,1 Hz, 4H, H$_4$-pz). ^{13}C NMR (100.6 MHz, acetone-d_6): 143.8 (C$_5$-pz), 139.2, 136.2, 131.3, 129.9 (C$_3$-pz), 129.6, 106.6 (C$_4$-pz), C$_\alpha$ not obsd. HRMS-ESI(+) (m/z): calcd for $C_{38}H_{32}N_8Ag$ [M − PF$_6$]$^+$, 707.1801; found, 707.1773. ESI(+) MS {m/z (rel int %), [assignment]$^+$}: 707 (68) [AgL$^1_2$]$^+$, 448 (100), [Ag(CH$_3$CN)(L^1)]$^+$; 407 (71), [AgL^1]$^+$; 233, [L^1]$^+$. Crystals suitable for X-ray structural studies were grown by layering an acetone solution with Et$_2$O and allowing the solvents to slowly diffuse.

{Ag[(pz)$_2$CHPh]$_2$}(PF$_6$) (2). Under a nitrogen atmosphere, a solution of 0.421 g (1.88 mmol) of PhCH(pz)$_2$ in 10 mL of THF was added by cannula to a solution of 0.237 g (0.938 mmol) of AgPF$_6$ in 10 mL of THF. A colorless precipitate formed within 10 min of stirring, and the resulting suspension was stirred 4 h. After separation of the colorless solid from the colorless solution by cannula filtration, the colorless solid was washed with two 5 mL portions of Et$_2$O and dried under vacuum to leave 0.545 g (83% yield) of {Ag[(pz)$_2$CHPh]$_2$}(PF$_6$) as a colorless solid. Mp: 245−247 °C (dec). Anal. Calcd (found) for $C_{26}H_{24}F_6N_8PAg$: C, 44.53 (44.45); H, 3.45 (3.01); 15.98 (16.05). ^{1}H NMR (300 MHz): 8.38 (d, J = 2 Hz, 4H, H$_5$-pz), 8.37 (s, 2H, C$_\alpha$H), 7.46 (br m, 6 H, Ph), 7.37 (d, J = 1 Hz, 4H, H$_3$-pz), 6.63 (br m, 4H, Ph), 6.53 (dd, J = 2,1 Hz, 4H, H$_4$-pz). ^{13}C NMR (75.4 MHz, acetone-d_6): 143.7 (C$_5$-pz), 136.7, 134.5, 130.0, 129.7 (C$_3$-pz), 127.3, 107.1 (C$_4$-pz), 75.8. HRMS-ESI(+) (m/ z): [M − PF$_6$]$^+$ calcd for $C_{26}H_{24}N_8Ag$, 555.1175; found, 555.1174. Crystals suitable for X-ray structural studies were grown by vapor diffusion of Et$_2$O into a CH$_2$Cl$_2$ solution of the compound.

{Ag[(pz)$_2$CHCH$_2$Ph]$_2$}(PF$_6$) (3). A solution of 0.111 g (0.466 mmol) of PhCH$_2$CH(pz)$_2$ in 10 mL of THF was added to a solution of 0.590 g (0.233 mmol) of AgPF$_6$ in 10 mL of THF under a nitrogen atmosphere. The resulting amber solution was stirred 4 h, and then solvent was removed by vacuum distillation. The colorless solid was washed with 5 mL of Et$_2$O and dried under vacuum to leave 0.137 g (81% yield) of {Ag[(pz)$_2$CHCH$_2$Ph]$_2$}(PF$_6$) as a colorless solid. Mp: 186−188 °C (dec). Anal. Calcd (found) for $C_{28}H_{28}N_8F_6PAg$: C, 46.13 (46.05); H, 3.87 (3.72); N, 15.37 (15.21). ^{1}H NMR (400 MHz): 8.10 (d, J = 2 Hz, 4H, H$_5$-pz), 7.87 (d, J = 1 Hz, 4H, H$_3$-pz), 7.38 (t, J = 8 Hz, 2H, C$_\alpha$H), 7.23 (br m, 10 H, Ph), 6.44 (dd, J = 2.1 Hz, 4H, H$_4$-pz), 4.30 (d, J = 8 Hz, 4H, CH$_2$). ^{13}C NMR (100.6 MHz, acetone-d_6): 143.8 (C$_5$-pz), 135.7, 133.3, 130.0, 129.4 (C$_3$-pz), 128.2, 107.2 (C$_4$-pz), 75.9, 40.7. HRMS-ESI(+) (m/z): [M − PF$_6$]$^+$ calcd for $C_{28}H_{28}N_8Ag$, 583.1488; found, 583.1473. ESI(+) MS {m/z (rel int %) [assignment]$^+$}: 583 (43), [M − PF$_6$]$^+$; 345 (41), [AgL^3]; 239 (100), [HL^3]; 171 (20), [HL^3 − pz]. Crystals of {Ag[(pz)$_2$CHCH$_2$Ph]$_2$}(PF$_6$)·CH$_2$Cl$_2$ suitable for X-ray structural studies were grown by layering a CH$_2$Cl$_2$ solution with hexanes and allowing the solvents to slowly diffuse.

Anal. Calcd (found) for $C_{29}H_{30}N_8F_6Cl_2PAg$, M·CH$_2Cl_2$: C, 42.77 (43.26); H, 3.71 (3.38); N, 13.76 (13.77).

Crystallography. X-ray Structure Determinations of {Ag-[(pz)$_2$CPh$_2$]$_2$}(PF$_6$)·C$_3$H$_6$O, 1·Acetone, Ag[(pz)$_2$CHPh]$_2$}(PF$_6$)·0.5CH$_2$Cl$_2$, 2·0.5CH$_2$Cl$_2$, and Ag[(pz)$_2$CHCH$_2$Ph]$_2$}(PF$_6$)·CH$_2$Cl$_2$, 3·CH$_2$Cl$_2$. Colorless block crystals of **1** and **2** and a colorless plate of **3** were each mounted onto the end of thin glass fibers using inert oil. X-ray intensity data from **1** was measured at 190(2) K, while those data from **2** and **3** were measured at 150(2) K on a Bruker SMART APEX CCD-based diffractometer (Mo Kα radiation, λ = 0.710 73 Å).[8] The raw data frames were integrated with SAINT+,[8] which also applied corrections for Lorentz and polarization effects. Final unit cell parameters were determined by least-squares refinement of 6659 reflections from the data set of **1**, of 5066 reflections from the data set of **2**, and of 8072 reflections from the data set of **3**, each with I > 5σ(I). Analysis of the data showed negligible crystal decay during each data collection. Empirical absorption corrections for each data set were applied with SADABS.[8]

Structure Refinement of {Ag[(pz)$_2$CPh$_2$]$_2$}(PF$_6$)·C$_3$H$_6$O, 1·Acetone. Structure solutions at 190 and 294 K (Supporting Information) (direct methods) and full-matrix least-squares refinement against F^2 were carried out with SHELXTL.[9] {Ag[(pz)$_2$-CPh$_2$]$_2$}(PF$_6$)·C$_3$H$_6$O crystallizes in the triclinic system. The space group $P\bar{1}$ was assumed and confirmed by successful solution and refinement of the data. The Ag atom of the cation and the P atom of the anion reside on crystallographic inversion centers. One acetone molecule/formula unit is disordered about an inversion center, and a restrained model incorporating two orientations was used. All non-hydrogen atoms were refined with anisotropic displacement parameters; hydrogen atoms were placed in idealized positions and included as riding atoms.
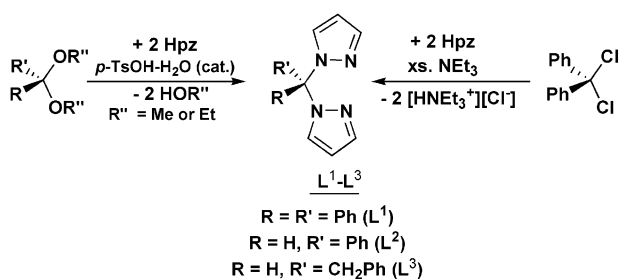
Structure Refinement of {Ag[(pz)$_2$CHPh]$_2$}(PF$_6$)·0.5CH$_2$Cl$_2$, 2·0.5CH$_2$Cl$_2$. Systematic absences in the intensity data were consistent with the space groups $P3_1$, $P3_2$, $P3_121$, and $P3_221$. Preliminary solutions confirmed the presence of a C_2 axis in the crystal, leaving the enantiomorphous pair $P3_121/P3_221$. Solutions were obtained in both space groups. The space group $P3_221$ resulted in a Flack parameter of 0.00(3). Refinement in $P3_121$ gave a Flack parameter of 0.9(2), confirming $P3_221$ as the correct space group. Final R values were also lower in $P3_221$. The final refinement was carried out in $P3_221$. Structure solutions were obtained by a combination of direct methods and difference Fourier syntheses, and refinement was carried out by full-matrix least squares against F^2, using SHELXTL.[9] The {Ag[(pz)$_2$CHPh]$_2$}$^+$ complex has crystallographically imposed 2-fold symmetry. The disordered PF$_6$$^-$ anion was modeled in two positions with equal weighting. A methylene chloride molecule is also equally disordered over two positions. Eventually all non-hydrogen atoms were refined with anisotropic displacement parameters; hydrogen atoms were placed in geometrically idealized positions and included as riding atoms with refined isotropic displacement parameters.

Structure Refinement of {Ag[(pz)$_2$CHCH$_2$Ph]$_2$}(PF$_6$)·CH$_2$Cl$_2$, 3·CH$_2$Cl$_2$. Systematic absences in the intensity data uniquely determined the space group *Pbca*. The structure was solved by a combination of direct methods and difference Fourier syntheses and refined by full-matrix least squares against F^2, using SHELX-TL.[9] All atoms reside on positions of general crystallographic symmetry. The {Ag[(pz)$_2$CHCH$_2$Ph]$_2$}$^+$ cation, PF$_6$$^-$ anion, and

(8) *SMART Version 5.625, SAINT+ Version 6.22, and SADABS Version 2.03*; Bruker Analytical X-ray Systems, Inc.: Madison, WI, 2001.
(9) Sheldrick, G. M. *SHELXTL Version 6.1*; Bruker Analytical X-ray Systems, Inc.: Madison, WI, 2000.
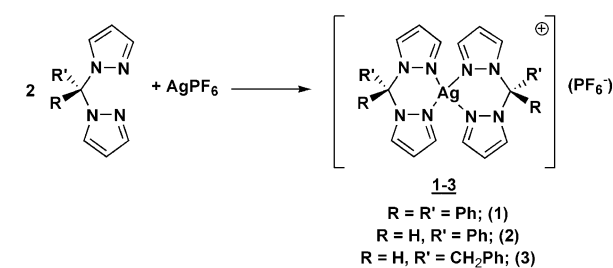
Scheme 1

Scheme 2

L^1-L^3

R = R' = Ph (L^1)
R = H, R' = Ph (L^2)
R = H, R' = CH_2Ph (L^3)

1-3

R = R' = Ph; (1)
R = H, R' = Ph; (2)
R = H, R' = CH_2Ph; (3)

included CH_2Cl_2 solvent are all afflicted by disorder. The benzyl group {C4−C66} of the cation is equally disordered over two nearby positions. The C_6 rings of both components were refined as rigid hexagons. The PF_6^- anion is disordered over two closely spaced positions in an approximate 60/40 ratio. A CH_2Cl_2 molecule of crystallization is also disordered over two closely spaced positions, in the ratio 80/20. A total of 29 geometric restraints were employed to assist in the refinement of the disordered atoms. The minor disorder component of the CH_2Cl_2 was refined isotropically; all other non-hydrogen atoms were refined with anisotropic displacement parameters. Hydrogen atoms were placed in geometrically idealized positions and included as riding atoms.

Results and Discussion

Syntheses. The synthetic methods used to prepare the ligands L^1−L^3 are outlined in Scheme 1. Both $PhCH(pz)_2$ (L^2) and $PhCH_2CH(pz)_2$ (L^3) were prepared in good to fair yields (75% and 38%, respectively) by the alcohol elimination reactions between pyrazole and either benzaldehyde dimethyl acetal or phenylacetaldehyde diethyl acetal, as appropriate. The ease of handling the air-stable, inexpensive, and commercially available reagents make the alcohol elimination reactions more favorable than the literature route to these compounds.[7] In the previously known route, CH_2-$(pz)_2$ (which must be prepared) is first reacted with butyllithium and then with the appropriate electrophile to give a product mixture that contains significant amounts of pyrazolyl-substituted compounds (from competing pyrazolyl deprotonation reactions). Compound L^1, on the other hand, was prepared in good yield (74%) by the reaction between dichlorodiphenylmethane, pyrazole, and triethylamine following a modification of the procedure used for the preparation of $Ph_2C(pz^{3Me})_2$.[10] In our hands, the known alcohol elimination route[11] involving benzophenone diethyl ketal and pyrazole provided a poor yield (<10% by NMR) of the desired product as a mixture with the starting material and benzophenone (hydrolysis byproduct). It should also be mentioned that attempts to prepare compound L^1 from the Peterson rearrangement reaction[6] between benzophenone, bis-(pyrazolyl)carbonyl, and $CoCl_2$ were unsuccessful as only trace quantity of L^1 was formed (NMR) regardless of the heating period (1−7 days).

The silver compounds 1−3 were isolated in approximately 70−80% yield as colorless solids that precipitated within

minutes of mixing THF solutions of the appropriate ligand and silver hexafluorophosphate (in a 2:1 mol ratio) (Scheme 2). These compounds appear to be indefinitely stable as solids toward ambient light; however, trace decomposition with the deposition of metallic silver has been observed for acetone-d_6 and $CDCl_3$ solutions upon prolonged (1 week) exposure to ambient light. The ^1H and ^{13}C NMR spectra show only one set of resonances that differ from the spectra of the free ligands by an upfield shift of the H_3-pz and one of the phenyl resonances of compounds 2 and 3, while the remainder of the resonances in each compound exhibit downfield shifts with respect to the free ligand. These observations are consistent with the known lability of related silver poly-(pyrazolyl)methane complexes and indicate that metal−arene interactions are nonexistent in solution.[12] The ESI(+) mass spectrum of each compound showed peaks corresponding to the $[AgL_2]^+$ cation.

Compounds 1−3 crystallize as solvates as noted in the Experimental Section and in Table 1. The geometry of the cations and labeling of atoms are given for each in Figures 3 and 4, while important bond distances and angles are provided in Table 2.

As can be seen in Figure 3, the silver center in 1 adopts an unusual square planar coordination environment as indicated by the sum of the four N−Ag−N angles which is 360°. The square planar geometry is distorted by the N(11)−Ag−N(21) bite angle of 74.44(6)° associated with the chelating ring. The Ag−N bond distances (the silver atom resides on an inversion center) of 2.356(2) and 2.367(2) Å fall within the range of 2.28−2.50 Å found in {Ag(κ^2-m-$C_6H_4[C(pz)_2(2$-py)]$)_2$}(PF_6), {Ag(κ^2-$C_6H_5[C(pz)_2(2$-py)]$)_2$}-(PF_6),[3] and related systems.[12b,13,17]

The proximity of phenyl groups above and below the AgN_4 core enforces the unusual square planar coordination geometry about the metal center. The shortest silver−carbon

(10) Shiu, K.-B.; Yeh, L.-Y.; Peng, S. M.; Cheng, M. C. *J. Organomet. Chem.* **1993**, *460*, 203.

(11) Tsuji, S.; Swenson, D. C.; Jordan, R. F. *Organometallics* **1999**, *18*, 4758.

(12) (a) Reger, D. L.; Gardinier, J. R.; Grattan, T. C.; Smith, M. D. *New J. Chem.* **2003**, 1670. (b) Reger, D. L.; Gardinier, J. R.; Semeniuc, R. F.; Smith, M. D. *J. Chem. Soc., Dalton Trans.* **2003**, 1712.

(13) Reger, D. L.; Brown, K. J.; Gardinier, J. R.; Smith, M. D. *Organometallics* **2003** *22*, 4973.

(14) (a) Lindeman, S. V.; Rathore, R.; Kochi, J. K. *Inorg. Chem.* **2000**, *39*, 5707. (b) Munakata, M.; Wu, L. P.; Ning, G. L.; Kuroda-Sowa, T.; Maekawa, M.; Suenaga, Y.; Maeno, N. *J. Am. Chem. Soc.* **1999**, *121*, 4968. (c) Munakata, M.; Wu, L. P.; Sugimoto, K.; Kuroda-Sowa, T.; Maekawa, M.; Suenaga, Y.; Maeno, N.; Fujita, M. *Inorg. Chem.* **1999**, *38*, 5674.

(15) Cotton, F. A.; Frenz, B. A.; Murillo, C. A. *J. Am. Chem. Soc.* **1975**, *97* (8), 2118.

(16) Cremer, D.; Pople, J. A. *J. Am. Chem. Soc.* **1975**, *97* (6), 1354.

(17) Lorenzotti, A.; Bonati, F.; Cingolani, A.; Lobbia, G. G.; Leonesi, D.; Bovio, B. *Inorg. Chim. Acta* **1990**, *170*, 199.
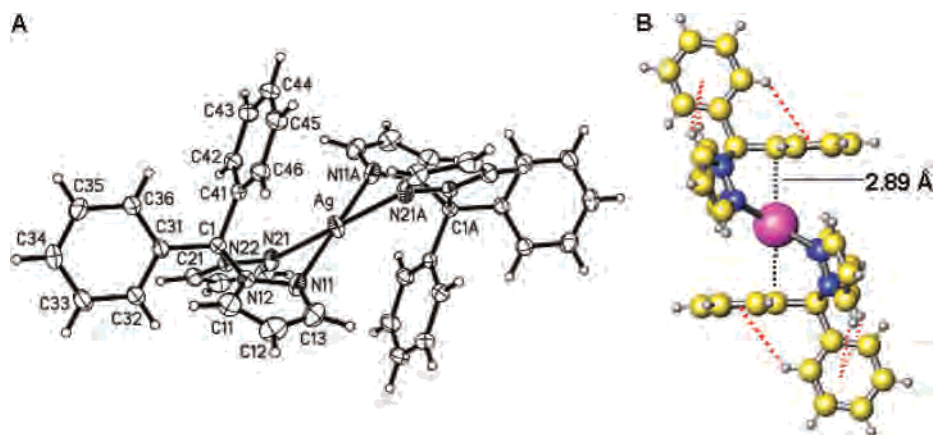
Figure 3. (A) Molecular geometry of the cation in {Ag[(pz)₂CPh₂]₂}(PF₆)·C₃H₆O, **1**·acetone, with 40% probability ellipsoids and (B) view depicting shortest silver−arene contact (2.89 Å) and intracationic noncovalent interactions (red dashed lines).
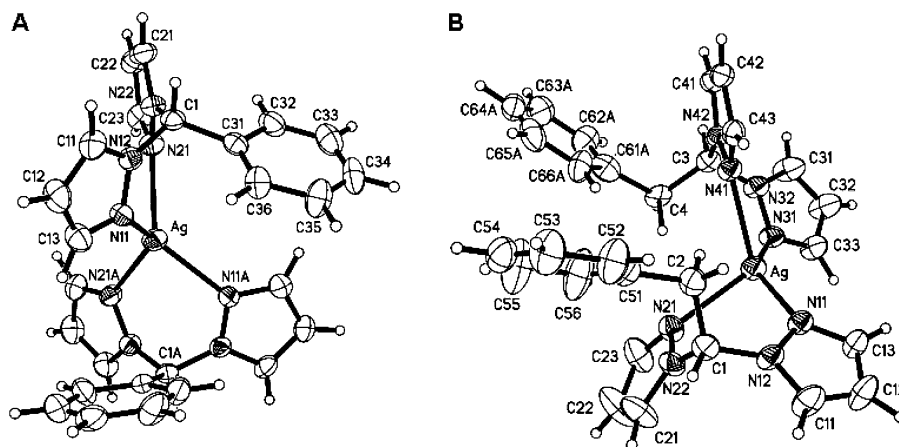
Figure 4. Molecular geometry of the cations in (A) {Ag[(pz)₂CHPh]₂}(PF₆)·0.5CH₂Cl₂, **2**·0.5CH₂Cl₂, and (B) {Ag[(pz)₂CH(CH₂Ph)]₂}(PF₆)·CH₂Cl₂, **3**·CH₂-Cl₂.

Table 1. Crystallographic Data for {Ag[(pz)₂CPh₂]₂}(PF₆)·C₃H₆O, **1**·Acetone, Ag[(pz)₂CHPh]₂}(PF₆)·0.5CH₂Cl₂, **2**·0.5CH₂Cl₂, and Ag[(pz)₂CHCH₂Ph]₂}(PF₆)·CH₂Cl₂, **3**·CH₂Cl₂

param	**1**·acetone	**2**·0.5CH₂Cl₂	**3**·CH₂Cl₂
emp formula	C₄₁H₃₈AgF₆N₈OP	C₂₆.₅H₂₅AgClF₆N₈P	C₂₉H₃₀AgCl₂F₆N₈P
fw	911.63	743.84	814.35
temp (K)	190(2)	150(2)	150(2)
space group	$P\bar{1}$	$P3_221$	$Pbca$
a (Å)	8.2996(6)	12.4420(4)	26.7828(14)
b (Å)	10.5681(7)	12.4420(4)	9.2886(5)
c (Å)	12.0865(8)	17.627(1)	27.116(1)
α (deg)	72.7520(10)	90	90
β (deg)	77.4620(10)	90	90
γ (deg)	80.7140(10)	120	90
V (Å³)	982.94(12)	2363.1(2)	6745.8(6)
Z	1	3	8
ρ_{calcd} (g/cm³)	1.540	1.568	1.604
abs coeff (mm⁻¹)	0.627	0.842	0.871
final R indices [I > 2σ(I)]	R1 = 0.0324, wR2 = 0.0870	R1 = 0.0281, wR2 = 0.0687	R1 = 0.0570 wR2 = 0.1444
R indices (all data)	R1 = 0.0349, wR2 = 0.0884	R1 = 0.0291, wR2 = 0.0692	R1 = 0.0618 wR2 = 0.1480

distance of 2.892(2) Å [Ag−C(41)] is shorter than the corresponding distance of 3.193 Å in {Ag(κ²-*m*-C₆H₄[C(pz)₂-(2-py)]₂)₂}(PF₆) and is just at the upper limit of the 2.4−2.9 Å range found in other compounds suggested to have η¹-silver(I)···arene π interactions.[14] This silver−carbon distance increases to 2.921(2) Å (above the Ag···π cutoff) in the room-temperature crystal structure (see Supporting Informa-

tion) which underscores the weakness of the interaction (if there is one).

The geometry of the ligand **L¹** appears to be constant regardless of the metal system to which it is bound as evidenced by inspecting the structures of **1** and [Ph₂C(pz)₂]-PdCl₂.[11] As originally pointed out by Cotton and co-workers,[15] in the related [Ph₂B(pz)₂]Mo(allyl)(CO)₃ ligand

Table 2. Selected Bond Lengths and Angles for Compounds 1−3

	compd **1**[a]	compd **2**	compd **3**		
			Bond Distances (Å)		
Ag−N(11)	2.367(2)	2.300(2)	2.243(4)	Ag−N(31)	2.273(5)
Ag−N(21)	2.356(2)	2.337(3)	2.419(5)	Ag−N(41)	2.408(5)
N(11)−N(12)	1.358(2)	1.351(4)	1.359(6)	N(31)−N(32)	1.355(6)
N(21)−N(22)	1.363(2)	1.353(4)	1.354(6)	N(41)−N(42)	1.359(6)
C(1)−N(12)	1.487(2)	1.457(4)	1.458(7)	C(3)−N(32)	1.450(7)
C(1)−N(22)	1.479(2)	1.449(4)	1.447(7)	C(3)−N(42)	1.454(7)
			Bond Angles (deg)		
N(11)−Ag−N(21)	74.44(6)	83.97(9)	85.1 (2)	N(31)−Ag−N(41)	84.6(2)
N(11)−Ag−N(21a)	105.56(6)	123.56	119.2(2)[b]	N(31)−Ag−N(21)	122.5(2)
N(12)−N(11)−Ag	117.4(1)	120.9(2)	121.9(3)	N(32)−N(31)−Ag	119.7(3)
C(13)−N(11)−Ag	133.9(1)	132.0(2)	130.2(4)	C(33)−N(31)−Ag	126.9(4)
C(13)−N(11)−N(12)	104.9(2)	104.3(2)	105.5(4)	C(33)−N(31)−N(32)	105.5(5)
N(11)−N(12)−C(11)	110.53(15)	111.6(3)	110.1(5)	N(31)−N(32)−C(31)	110.2(5)
N(11)−N(12)−C(1)	118.93(13)	121.4(2)	121.6(4)	N(31)−N(32)−C(3)	121.8(4)
C(11)−N(12)−C(1)	130.19(15)	127.0(3)	128.3(5)	C(31)−N(32)−C(3)	128.0(5)
N(22)−C(1)−N(12)	108.92(12)	111.5(3)	110.0(5)	N(42)−C(3)−N(32)	111.3(5)
N(21)−N(22)−C(1)	118.78(14)	121.8(3)	121.0(4)	N(41)−N(42)−C(3)	121.1(4)
C(21)−N(22)−C(1)	130.22(14)	126.4(3)	128.4(6)	C(41)−N(42)−C(3)	127.5(5)
C(21)−N(22)−N(21)	110.32(15)	111.2(3)	110.5(6)	C(41)−N(42)−N(41)	111.3(4)
N(22)−N(21)−Ag	118.51(11)	119.5(2)	116.3(3)	N(42)−N(41)−Ag	119.9(3)
C(23)−N(21)−N(22)	105.39(16)	104.5(3)	105.3(5)	C(43)−N(41)−N(42)	105.1(4)
C(23)−N(21)−Ag	135.74(13)	135.0(2)	131.0(4)	C(43)−N(41)−Ag	134.1(4)

[a] 190 K. [b] N(11)−Ag−N(41).

system, any other arrangement of phenyl groups in the complex (such as to promote phenyl CH−Mo agostic interactions) is prevented by steric interactions between aromatic hydrogens. Therefore, the steric congestion about the quarternary carbon combined with the additional favorable energetics associated with intracationic noncovalent interactions (Figure 3b and Supporting Information) in the present system contributes to the close Ag−aryl contact as opposed to any significant cation⋯π interaction.

The nitrogen atoms bonded to silver in **2** (Figure 4a) reside at the corners of a distorted tetrahedron with Ag−N bond distances (the silver atom resides on an inversion center) of 2.300(2) and 2.337(3) Å. The largest distortion from tetrahedral geometry is the N(11)−Ag−N(21) bite angle of 84.0° associated with the chelating ligand. The torsion angle between the two mean planes defined by N(11), Ag, and N(21) and its symmetry-related counterpart N(11a), Ag, and N(21a) in **2** is 84.7°. A torsion angle of 90° is expected for a perfect tetrahedron whereas a torsion angle of 0° is expected for a square planar arrangement as found in the case of compound **1**.

The coordination geometry about silver in **3** is distorted tetrahedral (Figure 4b), and contrary to the schematic depicted in Figure 2, there is no close Ag−arene contact. The four Ag−N bond distances in **3** show a disparity with two short [2.243(4) and 2.273(5) Å for Ag−N(11) and Ag−N(31)] and two long [2.419(5) and 2.408(5) Å for Ag−N(21) and Ag−N(41)] Ag−N bonds. Of the three title compounds **1**−**3**, compound **3** has the largest average N−Ag−N bite angle for the chelate ring(s) at an average value of 84.8°. The torsion angle between the two mean planes defined by N(11)−Ag−N(21) and N(31)−Ag−N(41) is 90.2°; however, the tetrahedron is further distorted by a 19.0° pivot of the mean N(31)−Ag−N(41) plane toward N(21).

Analysis of the arrangements of the AgN₄C chelate rings in these three structures shows that **1** adopts a boat config-

uration (as shown previously with complexes of Ph₂Cpz₂[11] or (Ph₂Bpz₂⁻)[15] ligands), while compounds **2** and **3** adopt conformations between a boat and half-boat geometry. These conclusions are supported by the data in Table 3 showing both the fold angles and Cremer−Pople ring puckering parameters[16] for compounds **1**−**3** and several related derivatives.[12b,13,17] By examination of either set of parameters given in Table 3 for a number of structurally characterized bis(pyrazolyl)methane complexes, it is evident that there is a trend correlating the steric demands of the substituents bound to the central methine carbon and the tendency toward adopting a boat conformation. The more bulky aryl group substituents bound to the central methine carbon have more acute fold angles involving silver (as defined in Table 3) and, as a consequence, exhibit a greater degree of boat character than those with fewer aryls. Thus, the fold angles decrease and a greater boat character is observed in the order of 172.4/173.4° for {Ag[(pz)₂CMe₂]₂⁺} < 164.1/165.4° for {Ag[(pz)₂CH(CH₂Ph)]₂⁺}(**3**) < 160.3° for {Ag[(pz)₂CHPh]₂⁺} (**2**) < 136.9° for {Ag[(pz)₂CPh₂]₂⁺} (**1**).

Supramolecular Structures. In both the 190 and 293 K (Supporting Information) structures, the cations in **1** aggregate into polymeric chains (Figure 5) along the crystallographic a-axis as a result of CH⋯π interactions between the phenyl group proximal to silver of one cation which acts as a hydrogen donor to the π clouds of the two pyrazolyl acceptors of an adjacent cation.[18,19] Interestingly, the polymeric supramolecular structure in **1** at 190 and 293 K is in contrast to the 294 K structures of {Ag(κ²-C₆H₅[C(pz)₂(2-py)])₂}(PF₆) and {Ag(κ²-m-C₆H₄[C(pz)₂(2-py)]₂)₂}(PF₆), whose cations were organized into quasi-inorganic−organic layered
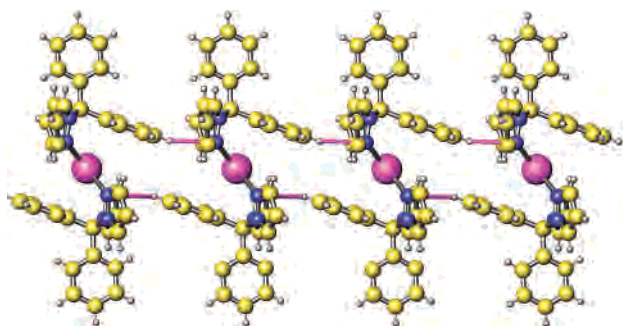
(18) Takahashi, H.; Tsuboyama, S.; Umezawa, Y.; Honda, K.; Nishio, M. *Tetrahedron* **2000**, *56*, 6185.
(19) Grepioni, F.; Cojazzi, G.; Draper, S. M.; Scully, N.; Braga, D. *Organometallics* **1998**, *17*, 296.

Table 3. Coordination Geometries and AgN$_4$C Ring Puckering Parameters in Various Silver Di(pyrazolyl)Methane Complexes

cation	coord environ	fold		Cremer−Pople params[c]			ref
		AgNN[a]	NNC[b]	Q	θ (deg)	ϕ (deg)	
{Ag(C$_6$H$_5$[C(pz)$_2$(2-py)])$_2$$^+$}^{d}	sq pl	135.4	130.4	na	na	na	3
{Ag[(pz)$_2$CPh$_2$]$_2$$^+$} (**1**)^d (190 K)	sq pl	136.4	127.9	1.090	101.56	184.2	j
{Ag[(pz)$_2$CPh$_2$]$_2$$^+$} (**1**)^d (293 K)	sq pl	136.9	128.6	1.081	101.57	184.6	
{Ag(m-C$_6$H$_4$[C(pz)$_2$(2-py)]$_2$)$_2$$^+$}^{d,g}	sq pl	147.7	128.6	0.910	96.90	181.8	3
{Fe[C$_5$H$_4$CH(pz)$_2$]$_2$Ag·OEt$_2$$^+$}$_n$^{d,h}	tet	154.0	124.5	0.823	88.30	178.5	13
{Ag[(pz)$_2$CHPh]$_2$$^+$} (**2**)^d	tet	160.3	124.8	0.736	87.62	180.5	j
{Ag$_2$(μ-[(pz)$_2$CH]$_2$CH$_2$)$_2$$^+$}^{d,g}	tet	160.4	126.9	0.726	87.20	172.3	12b
{Fe[C$_5$H$_4$CH(pz)$_2$]$_2$Ag$^+$}$_n$^{d,i}	tet	161.9	121.8	0.741	84.13	189.9	13
{Ag[(pz)$_2$CHCH$_2$Ph]$_2$$^+$} (**3**)^d	tet	164.1	121.4	0.712	82.64	171.9	j
		165.4	123.0	0.697	83.08	184.3	
{Ag$_2$(μ-[(pz)$_2$CH]$_2$CH$_2$)$_2$$^+$}^{e,g}	tet	167.6	121.1	0.669	79.00	178.7	12b
{Ag[(pz)$_2$CMe$_2$]$_2$$^+$}^{f}	tet	172.4	121.4	0.634	72.44	174.5	17
		173.4	120.9	0.633	73.23	186.6	

^{a} Fold AgNN is the angle defined by points connecting silver and the centroid between N(11) and N(21) and the centroid between N(12) and N(22), each of which lies on a plane bisecting AgN$_4$C chelate ring. ^{b} Fold CNN is similar but with the C atom replacing Ag as one point. ^{c} Reference 16. na: calculations not available due to extensive ligand disorder. Ideal boat has θ = 90 and ϕ = 180/0; ideal half-boat has θ = 54.7 and ϕ = 180/0. ^{d} PF$_6$$^-$ salt. ^{e} CF$_3$SO$_3$$^-$ salt. ^{f} ClO$_4$$^-$ salt. ^{g} One of two independent Ag sites. ^{h} Helical form. ^{i} Nonhelical form. ^{j} This work.

Figure 5. Polymeric chains of cations in {Ag[(pz)$_2$CPh$_2$]$_2$}(PF$_6$)·C$_3$H$_6$O, **1**·acetone, formed via CH···π interactions (pink lines).

Table 4. Summary of Noncovalent Interactions in {Ag[(pz)$_2$CHPh]$_2$}(PF$_6$)·0.5CH$_2$Cl$_2$, **2**·0.5CH$_2$Cl$_2$

donor (D)···acceptor (Å)	H···A (Å)	C(H)···A (deg)
C(1)H(1)···F(2)	2.36	156.6
C(1)H(1)···F(2a)	2.44	157.1
C(1)H(1)···F(5)	2.43	146.1
C(1)H(1)···F(6)	2.50	147.8
C(11)H(11)···F(2)	2.48	138.5
C(21)H(21)···F(6)	2.50	136.7
C(22)H(22)···F(5)	2.45	129.7
C(34)H(34)···F(3)	2.40	130.3
C(13)H(13)···Ct[C(33)]^a	3.20	134.4
C(33)H(33)···Ct[N(11)]	3.12	121.1
C(33)H(33)···Ct[N(21)]	2.97	134.7

^{a} Ct refers to centroid of the arene ring that contains the element denoted in brackets.

three-dimensional supramolecular structures by a combination of weak CH···π[18] *and CH···F interactions.*[19]

The cations in **2** are arranged into helical chains by CH···F interactions as shown in Figure 6, where the hexafluorophosphate anion serves as a bridge connecting adjacent cations. In particular, the acidic methine hydrogen participates in a trifurcated interaction with F(2), F(5), and F(6) of the hexafluorophosphate anion where the geometry of each component of this interaction is given in Table 4. It should be noted that while the hexafluorophosphate anion is disordered over two nearby positions, the proximity of the methine hydrogen [CH(1)] to each disorder component of the bridging atom F(2) is 2.36 and 2.44 Å, respectively, which are each well below the 2.6 Å proposed limit for weak

CH···F bonding interactions.[19] The helical chains can be generated by considering only the interaction between the methine hydrogen and F(2), while the remainder of the CH···F interactions involving F(5), F(6), and C(34)H-(34)···F(3) that are below the 2.6 Å cutoff (Table 4) help support both the helical arrangement and the overall three-dimensional supramolecular structure which is that of a close-packed network of helices (Figure 7). The helices are arranged in a close-packed network by a combination of the aforementioned CH···F interactions and by two types of CH···π interactions between the phenyl and pyrazolyl groups. In the first CH···π interaction, the pyrazolyl group acts as a hydrogen donor [H(13)], while the phenyl group acts as an acceptor [C(13)H(13)···centroid: 3.198 Å, 134.36°]. The second CH···π interaction is a bifurcated one in which the phenyl group acts as a hydrogen donor to the π clouds of two pyrazolyl rings of one adjacent cation. Specifically, H(33) of the phenyl group is directed toward the centroids (Ct) of the pyrazolyl rings containing N(11) and N(21) of an adjacent cation. The geometry of the interaction is such that the C(33)H(33)···Ct[N(11)] distance and angle of 3.12 Å and 121.1° along with the C(33)H(33)···Ct[N(21)] distance and angle of 2.97 Å and 134.7° are each within the typical range for a CH···π interaction (vide supra).[18]

Compound **3** appears to form a layered structure (Figure 8) as a result of numerous short CH···F interactions (<2.6 Å) and a CH···π interaction between a phenyl group hydrogen donor [H(42)] and a pyrazolyl group [containing N(31)] acceptor [C(42)H(42)···centroid 2.89 Å, 141.5°]. Unfortunately, a full examination of the supramolecular structure of **3** is precluded as a result of the disorder of one benzyl group (vide supra) in addition to that affecting both the PF$_6$$^-$ anion and the solvent of crystallization.

Conclusions

We have prepared three bis(pyrazolyl)methane ligands that contain varying degrees of steric bulk around the central carbon atom of the ligand. In the case of Ph$_2$C(pz)$_2$, **L^1**, the steric constraints imposed by the aryl groups enforce an unusual square planar conformation in the silver hexafluo-
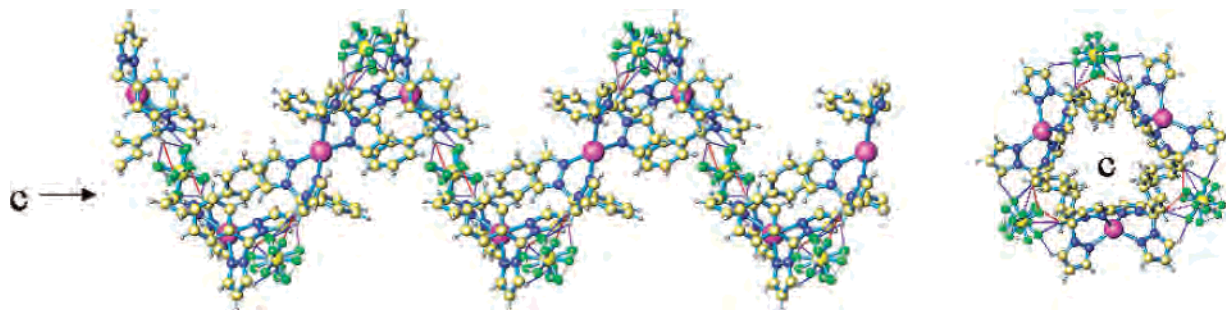
Figure 6. Helical chains in {Ag[(pz)$_2$CHPh]$_2$}(PF$_6$)·0.5CH$_2$Cl$_2$, **2**·0.5CH$_2$Cl$_2$. Views are perpendicular to the *c*-axis (left) and along the *c*-axis (right).
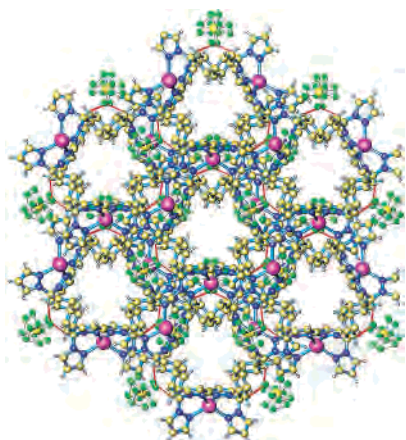
Figure 7. Close packing of helices in {Ag[(pz)$_2$CHPh]$_2$}(PF$_6$)·0.5CH$_2$-Cl$_2$, **2**·0.5CH$_2$Cl$_2$. Solvent (not shown) resides in channels created by helices.
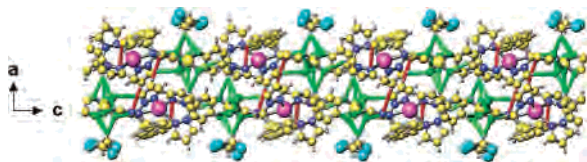
Figure 8. View of the side of a sheet in **3** (down *b*-axis) assembled by CH⋯F (green lines) and CH⋯π interactions (red lines).

rophosphate complex. This same effect was also observed in the related bis(pyrazolyl)(2-pyridyl)methane−aryl complexes, {Ag(κ^2-*m*-C$_6$H$_4$[C(pz)$_2$(2-py)]$_2$)$_2$}(PF$_6$) and {Ag-(C$_6$H$_5$[C(pz)$_2$(2-py)])$_2$}(PF$_6$). One consequence of this arrangement is that the AgN$_4$C chelate rings adopt boat configurations. When the steric congestion about the methine carbon is alleviated as in either PhCH(pz)$_2$, **L^2**, or PhCH$_2$C-(pz)$_2$, **L^3**, the silver(1) centers adopt the more familiar tetrahedral coordination geometry and the AgN$_4$C rings are no longer in the boat conformation; rather they adopt conformations between a full boat and half boat. Qualitatively, the boat conformation is favored for bulky groups bound to the methine carbon whereas the less sterically demanding substituents favor the half-boat conformation. The general order found by a comparison of the fold angle involving the metal atom of the AgN$_4$C chelate ring for a number of different structurally characterized silver bis-(pyrazolyl)methane complexes is (alkyl)(H)C(pz)$_2$ > (aryl)-(H)C(pz)$_2$ > (aryl)$_2$C(pz)$_2$.

The supramolecular structures of the three complexes {Ag-[(pz)$_2$CPh$_2$]$_2$}(PF$_6$), **1**·acetone, {Ag[(pz)$_2$CHPh]$_2$}(PF$_6$)·0.5CH$_2$-Cl$_2$, **2**·0.5CH$_2$Cl$_2$, and {Ag[(pz)$_2$CHCH$_2$Ph]$_2$}(PF$_6$)·CH$_2$Cl$_2$, **3**·CH$_2$Cl$_2$ are assembled as a result of CH⋯π interactions and for **2**·0.5CH$_2$Cl$_2$ and **3**·CH$_2$Cl$_2$ also by CH⋯F interactions such that polymeric chains of cations form in the case of compound **1**, a closed-packed helical network of cations is found for **2**, and sheets of a cations are found in **3**. It is likely that the supramolecular organization has a minor contribution to the perturbing the coordination geometry about silver; given the large variety of supramolecular structures observed for the known silver pyrazolylmethane complexes, it is evident that the coordination geometry about silver is primarily dictated by the steric demands of the ligand.

Finally, given that no significant Ag⋯π interactions were observed in **1**−**3**, {Ag(κ^2-*m*-C$_6$H$_4$[C(pz)$_2$(2-py)]$_2$)$_2$}(PF$_6$), or {Ag(C$_6$H$_5$[C(pz)$_2$(2-py)])$_2$}(PF$_6$) but were observed in the coordination polymer {*o*-C$_6$H$_4$[CH$_2$OCH$_2$C(3-Phpz)$_3$]$_2$Ag$_2$-(acetone)(BF$_4$)$_2$}$_n$, it is clear that designing ligands that place an arene group in proximity to silver(I) is not enough to ensure a cation⋯π interaction. Rather, it is also necessary for the silver center to have an available coordination site. The tetracoordination of the silver(I) observed for the former five compounds prevents cation⋯π arene interactions, whereas in the latter coordination polymer the tricoordinate silver expands its coordination sphere by η^2-bonding to a neighboring phenyl ring.

Supporting Information Available: Crystallographic information files (CIF's) for **1**·acetone at 293 and at 190 K, **2**·0.5CH$_2$Cl$_2$, and **3**·CH$_2$Cl$_2$ and full details of supramolecular interactions in **1**. This material is available free of charge via the Internet at http://pubs.acs.org.

IC0497174